Characterization and modeling of 2D-glass micro-machining by spark-assisted chemical engraving (SACE) with constant velocity

2008 J. Micromech. Microeng. 18 065016

(http://iopscience.iop.org/0960-1317/18/6/065016)

J. Micromech. Microeng. **18** (2008) 065016 (9pp) doi:10.1088/0960-1317/18/6/065016

Characterization and modeling of 2D-glass micro-machining by spark-assisted chemical engraving (SACE) with constant velocity

Tohid Fatanat Didar, Ali Dolatabadi and Rolf Wüthrich

Department of Mechanical and Industrial Engineering, Concordia University, Montreal, QC H3G 1M8, Canada

E-mail: wuthrich@encs.concordia.ca

Received 29 January 2008, in final form 8 April 2008
Published 9 May 2008
Online at stacks.iop.org/JMM/18/065016

Abstract
Spark-assisted chemical engraving (SACE) is an unconventional micro-machining technology based on electrochemical discharge used for micro-machining nonconductive materials. SACE 2D micro-machining with constant speed was used to machine micro-channels in glass. Parameters affecting the quality and geometry of the micro-channels machined by SACE technology with constant velocity were presented and the effect of each of the parameters was assessed. The effect of chemical etching on the geometry of micro-channels under different machining conditions has been studied, and a model is proposed for characterization of the micro-channels as a function of machining voltage and applied speed.

1. Introduction

Spark-assisted chemical engraving (SACE) is a promising micro-machining technology for the low-cost machining of holes and channels in nonconducting materials, such as glass and some ceramics [1, 2]. The machining takes place in an electro-chemical cell where the cathode is used as a tool and the anode as a counter-electrode. When a voltage higher than a critical value, called critical voltage, is applied, bubbles grow so dense on the tool electrode that they coalesce into a gas film; this has been identified as one of the key parameters for machining repeatability [3]. Electrical discharges take place between the tool electrode and the electrolyte. When the tool electrode is brought in close vicinity (less than 25 μm for glass [1]) of the substrate, machining takes place. The exact mechanism of material removal is still not completely understood; however, it can be attributed to thermal melting due to local heating by the electrochemical discharges and some chemical effects [1, 4–6].

Micro-hole drilling with gravity feed was the very first application presented for SACE; however, several other applications have been reported. Recently, the quality of the obtained micro-holes as a function of applied voltage and drilled depth has been characterized by Maillard *et al* [7]. It is possible to perform 2D and 3D machining by moving the tool over the working piece [8–10]. This was first reported by Langen *et al* [11]. Later, Wüthrich and co-workers [11–13] reported micro-channels of 100 μm width and a few millimeters long. Recently, the effect of tool rotation and pulse voltage [14] and electrolyte composition [15] on the performance of 2D micro-machining have been reported. However, none of these studies was designed to improve understanding of the key mechanisms controlling the quality and geometry of micro-channels.

The quality and geometrical specifications of machined micro-channels have so far never been characterized systematically. As micro-channels play a vital role in MEMS, micro-fluidic or lab-on-a-chip devices, the quality of machined channels and the depth of the channels must be well controlled.

The present work provides a quantitative description of achievable geometrical tolerances and micro-channel quality using SACE constant velocity machining. The study focuses on the characterization of achievable geometrical tolerances as a function of the machining voltage and tool speed. The impact of chemical etching in 2D-SACE micro-machining is quantified. The machined micro-channels are characterized, and a phenomenological model for SACE constant-velocity

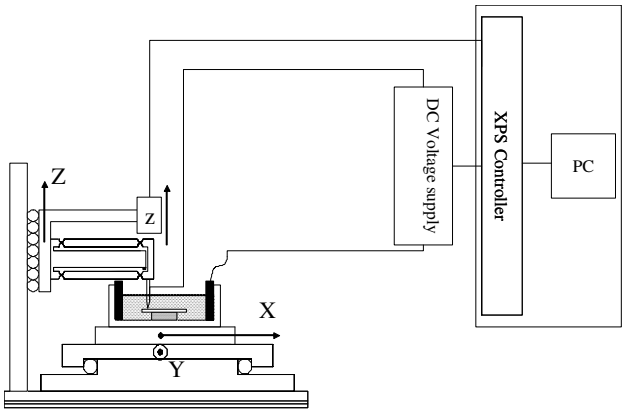

Figure 1. Schematic representation of the experimental setup used.

2D machining is proposed and was shown to have firm theoretical bases.

2. Experimental setup and procedure

2.1. Micro-machining setup

The experimental setup schematically shown in figure 1 is similar to the setup used by Maillard *et al* [7]; however, the present setup has the advantage of 3D motion, i.e., the drilling head can move simultaneously along the three axes to follow a 3D trajectory. The processing cell is mounted on an *XY* stage with the workpiece and on a *Z* stage the machining head with the fixed tool electrode. *XYZ* stages are from Newport® which are being controlled using an XPS motion controller from the same company. The machining head consists of a homemade flexible structure which allows detecting the glass surface for 2D machining. The electrolyte used in this work was 30 wt% NaOH. Its mean temperature was the ambient temperature before starting the machining in all experiments. The tool electrodes were cylindrical electrodes of 0.5 mm diameter in 316 L stainless steel. The shape of the electrodes was inspected prior to the machining with an optical microscope and, if necessary, corrected using emery paper. As a counter-electrode a large cylindrical ring (same diameter as the processing cell) in stainless steel was used. The workpieces were standard glass sample holders for optical microscopes with a thickness of 1 mm (Menzel–Glässer, a soda-lime glass). The processing cell was cylindrical with a diameter of 11 cm. The power source used in this work is a commercial power source Lambda Zup (60 V–3.5 A).

2.2. 2D machining procedure

In the first step, the machining head is positioned on the *XY* stage at the desired position. The *Z* stage is slowly moved down (at 200 μm s^{-1}) until the machining head touches the glass surface. This point will be the end point of the micro-channel. The *Z*-stage speed is chosen slow enough to get repeatability in the surface position detection smaller than 5 μm. When the glass surface is detected, the *Z* stage is moved up and then the *X* stage moves to obtain the desired channel length (15 mm). Then, the *Z* stage is moved down, according to the same procedure as the first point, to detect the second point of the channel. The two detected points will define a line in the *XZ* plane. Using these two points, the equation of a line is formed: the ideal trajectory. The ideal trajectory can only be followed for a surface which is completely smooth; the notion of a smooth surface is meaningless at micro-scale and any real surface exhibits defects at this scale. The glass samples used in the experiments are guaranteed by the manufacturer to have surface defects smaller than 1 μm. Therefore surface irregularities can be neglected and the ideal trajectory has to be modified only to take the machine error into account to avoid the machining tip touching the surface. This error is attributed to the system which is used for glass surface detection and is measured to be approximately 3 μm. The primary line is then shifted along the *Z*-axis in an amount equal to this error plus the desired tool distance from the glass surface. The shifted line, which is called the 'practical trajectory', is the trajectory followed by the machining tip (figure 2).

After finding the equation of the practical trajectory, the machine tip is moved to the first point of the practical trajectory, the voltage is switched on and the tip is moved along this trajectory. The magnitude of the velocity vector in the *XZ* plane is kept at a pre-specified constant value. When the tool reaches the last point of the practical trajectory, voltage is switched off and the process for 2D machining is finished.

The next step is to measure the depth of the channel. The procedure used to measure the machined micro-channel depth is as follows: ten points are chosen along the machined micro-channel, the machining tip is kept at a safe distance from the surface (about 3 mm) and moves through these points consecutively and on each point the tip moves along the *Z* axes until it touches the channel surface at which point the coordinate of the point is saved. Comparing this coordinate with the analogous point on the ideal trajectory, the depth of the micro-channel at that point is obtained. These points were chosen to be in the middle of the micro-channel (with

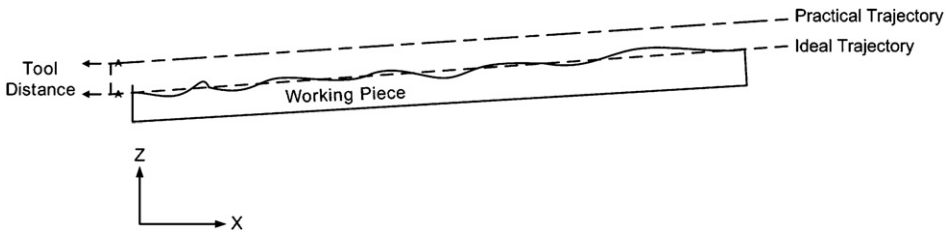

Figure 2. Schematic representation for 2D micro-machining with constant velocity.

2 mm distance from two ends) to avoid boundary effects. Since the tip itself has a finite thickness, the measured values have to be interpreted with care. These measured depth values were verified and confirmed using an optical microscope. To automate the procedures explained above, computer programs were developed using the TCL scripting language.

3. Results and discussion

Several parameters affect the quality and geometry of micro-channels fabricated by SACE technology with constant velocity, the most important of which are the tool speed, the applied voltage, the tool distance from the glass surface, the thickness of the electrolyte layer above the glass surface and tool travel length. It is very difficult to control the thickness of the electrolyte layer above the glass surface; therefore, this parameter was not used as a variable and in all the experiments the same amount of electrolyte was used. Various experiments were performed to find the effect of the other parameters on machined micro-channels. All the experiments were done with a tool distance of about 5 μm from the glass surface. Only in the experiments which were performed to study the effect of the tool distance from the glass surface, this distance was varied. In the following sections the results will be discussed including the quality of the machined channel and their geometrical characteristics.

3.1. Quality of the machined micro-channels

As the tool is moved above the glass surface for 2D micomachining, the first question is to find out the upper limit of velocity in which a micro-channel is formed. Whether a micro-channel is formed depends not only on the tool speed but also on the applied voltage and tool distance from the working piece. In some speeds it is not possible to have any micro-channel formation. This limit varies for different voltages; for example, in 28 V it is not possible to have any acceptable channel shape for speeds >40 μm s^{-1} and for 30 V this limit is >50 μm s^{-1}.

On the other hand, applying high voltages (more than 32 V) at low speeds results in an unsmooth channel surface with significant depth variation along the channel surface. The quality of the micro-channels deteriorates as the tool speed is decreased. This can be attributed to the poor material removal rate and accumulation of melted material inside the previous machined micro-channel surfaces.

In other cases it is possible to have a micro-channel with edges and surfaces of acceptable quality. Concerning the above-mentioned points, following contours can be distinguished as a function of the machining voltage and tool speed:

(1) *Well-defined linear channel edges and smooth channel surface.* This type of counters is a characteristic for low voltages with appropriate constant velocity. This format can be found in 28 V with tool speed ranging from 5 μm s^{-1} to 10 μm s^{-1} and in 30 V with tool speed ranging from 15 μm s^{-1} to 30 μm s^{-1} (figures 3(*a*), 4(*a*)).

(2) *Jagged outline contours with smooth channel surface.* This contour is observed for lower voltages (less than 32 V) with speeds lower than in the previous contour type. In this contour the micro-channel edges are jagged but the channel surface is still flat and smooth, as for example in 30 V when the speed is reduced to lower than 15 μm s^{-1} (figures 3(*b*), 4(*b*)).

(3) *Heat-affected edges with smooth channel surface.* This contour belongs to higher voltages (more than 32 V) with speeds high enough to remove the melted material. Under these conditions, the micro-channels will exhibit smooth channel surface but the channel boundaries are not well defined due to the effect of heat generation (figures 3(*c*), 4(*c*)).

(4) *Heat-affected edges with an unsmooth channel surface and thermal cracks.* When the speed is low at high voltages (32 V with speed less than 30 μm s^{-1} and 35 V with speed less than 40 μm s^{-1}), the edges are unclear and heat affected and the surface is not flat and smooth with thermal cracks (figures 3(*d*), 4(*d*)).

(5) *Deteriorated micro-channels (discretized boundaries with unsmooth surface and varying depth).* As the tool speed is increased the channel will be discretized and the inside surface will be very rough. For example in 28 V increasing the speeds above 40 μm s^{-1} will result in deteriorated micro-channels (figure 3(*e*)).

3.2. Geometry of the machined micro-channels

There are two main parameters in investigation of the geometry of the machined micro-channels: width and depth of the micro-channels. For a cylindrical stainless-steel tool of 0.5 mm in diameter used in all of the experiments, the width for all the micro-channels was measured to be approximately 700 μm. But the depth of the micro-channels varies as a function of all the mentioned parameters in section 3. In the following, the effect of these parameters on the micro-channels depth will be discussed.

3.2.1. Machining depth as a function of time with constant applied voltage and speed. According to the experiments, the depth of the machined channels varies as a function of time. Considering the machined channels on a working piece, the depth of the fourth micro-channel is more than the third one and so on. For a precise study of this effect an experiment was performed at a tool speed of 5 μm s^{-1} for a micro-channel of 15 mm length which lasted 50 min. Figure 5 shows the depth along different points of this micro-channel as a function of time required to drill this length. The results show that there is a meaningful relationship between the machining time and channel depth. As can be seen in figure 5, the micro-channel depth increases as a function of time with a constant rate. The main contributor to this phenomenon seems to be chemical etching. Chemical etching increases with a constant rate, depending on the applied voltage and tool speed. This has been explained in section 3.4.1 in more detail.

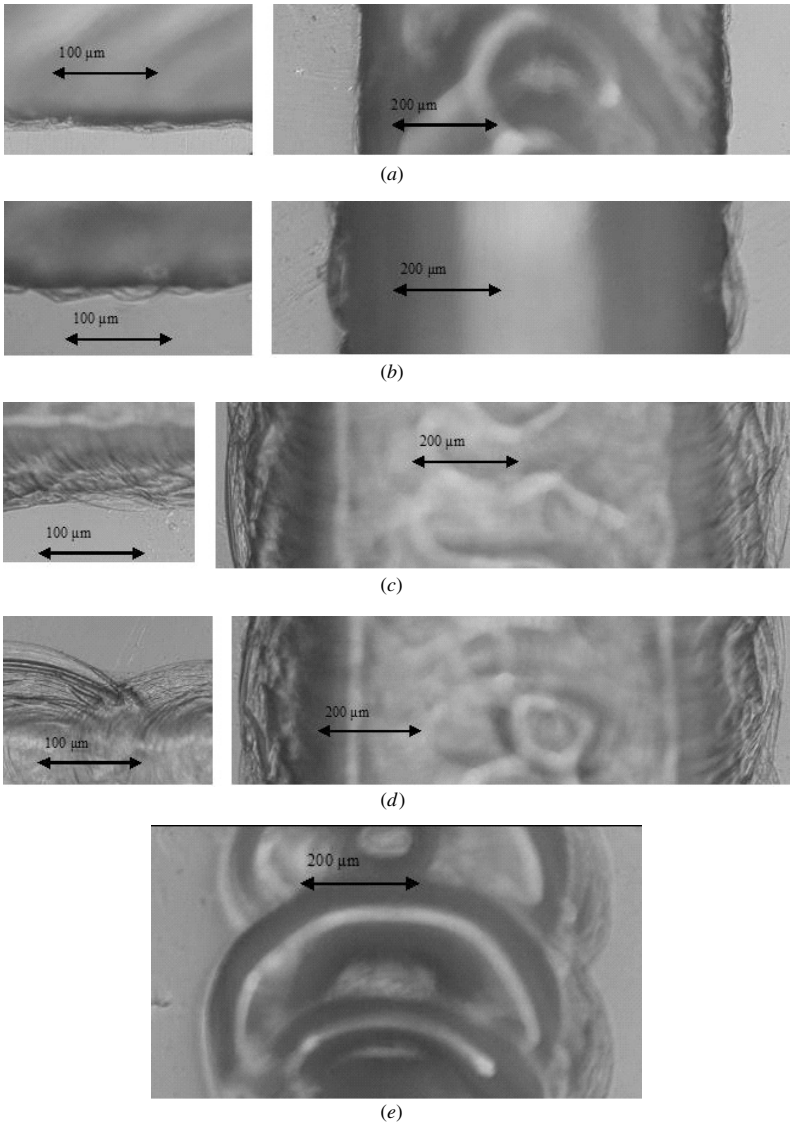

Figure 3. Channel contours: (*a*) well-defined linear channel edges and smooth channel surface, (*b*) jagged outline contours with smooth channel surface, (*c*) heat-affected edges with smooth channel surface, (*d*) heat-affected edges with rough channel surface, (*e*) deteriorated micro-channels.

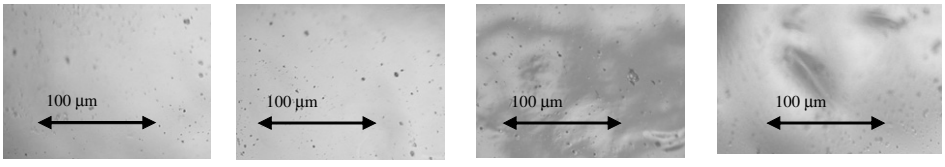

Figure 4. Quality of the surface of machined micro-channels: (*a*) channel surface for a well-defined edge, (*b*) channel surface for a jagged edge, (*c*) channel surface for a heat-affected edge, (*d*) rough channel surface with heat-affected boundaries.

3.2.2. Depth of the machined micro-channels as a function of voltage with constant applied speed. Higher voltages result in higher micro-channel depth. This statement is true up to 32 V. Applying voltages higher than 32 V at low speeds, as discussed in section 3.1, will not result in deeper micro-channels, but at high tool speeds, increasing the voltage results in deeper micro-channels which follow the same geometry as in voltages less than 32 V. Figure 6 shows the

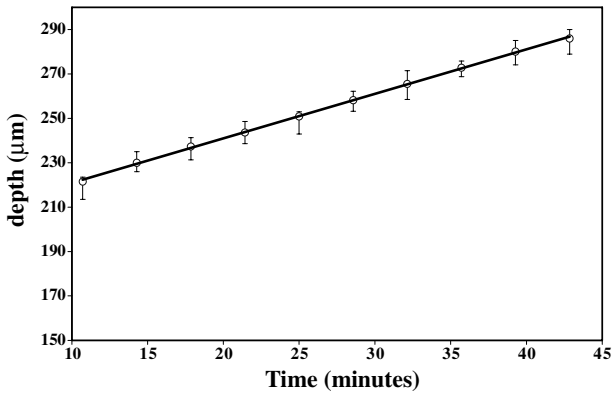

Figure 5. Micro-channel depth as a function of machining time in 28 V and 5 μm s^{-1}. Standard deviation calculated from a batch of four experiments.

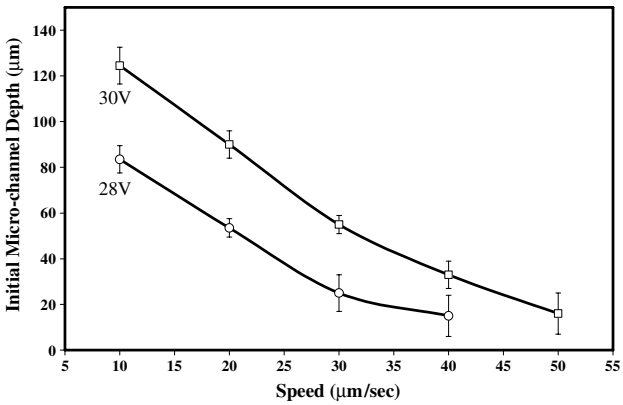

Figure 7. Initial micro-channel depth in 28 V and 30 V as a function of tool speed. Standard deviation calculated from a batch of five experiments.

effect of the increasing voltage at constant speed. This figure indicates the increasing trend of micro-channel depth with voltage.

3.2.3. Depth of the machined micro-channels as a function of speed with constant voltage. Horizontal tool speed plays the main role in micro-channel depth. Decreasing the speed in constant voltages results in deeper micro-channels, as shown in figure 7. Initial depth ($x = 0$) as a function of tool speed is shown in this figure in order to eliminate the effect of machining time on micro-channel depth. At 28 V, tool speeds more than 40 μm s^{-1} result in deteriorated micro-channels. So, the mean depth curve for 28 V has no meaning at speeds more than 40 μm s^{-1}.

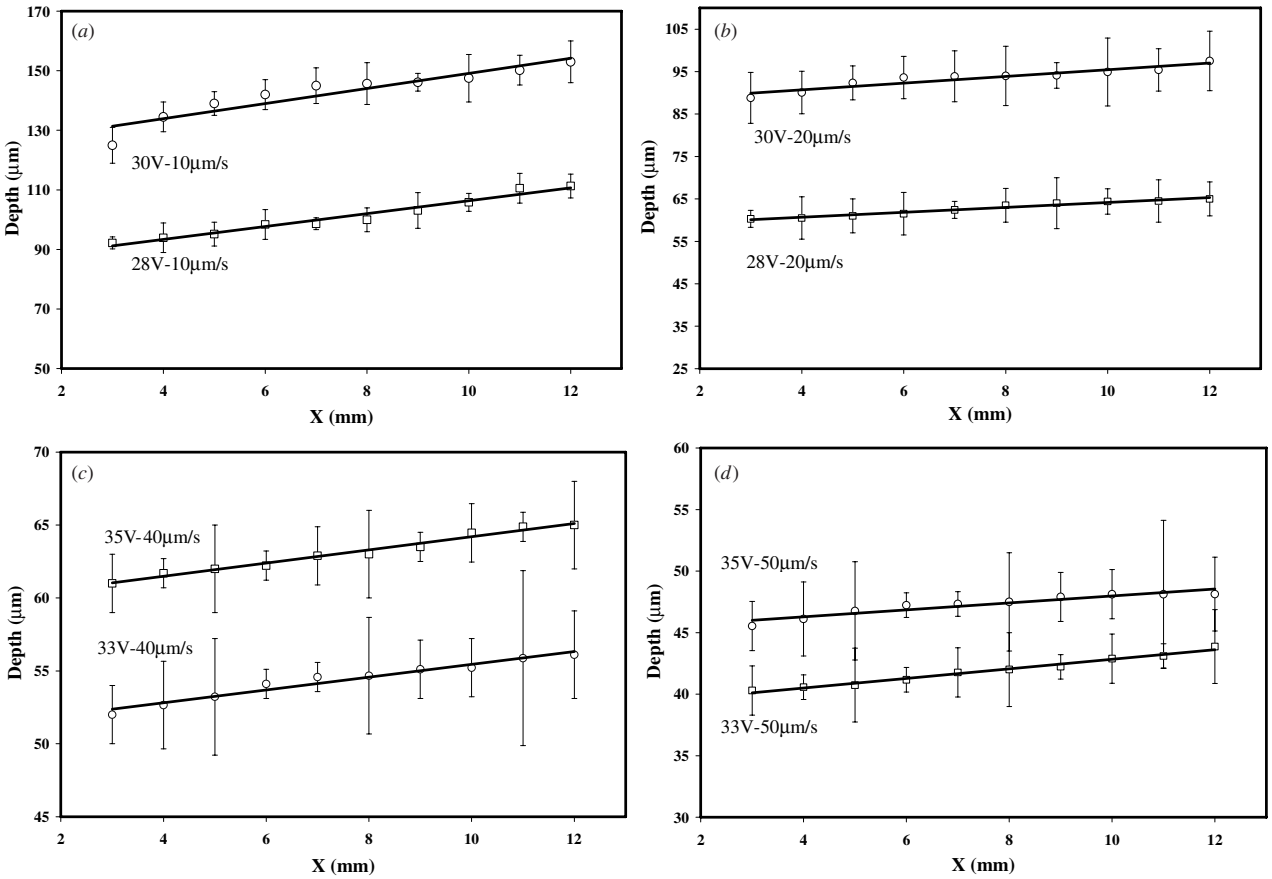

Figure 6. Micro-channel depth profile: (*a*) 28 V and 30 V at 10 μm s^{-1}, (*b*) 28 V and 30 V at 20 μm s^{-1}, (*c*) 33 V and 35 V at 40 μm s^{-1}, (*d*) 33 V and 35 V at 50 μm s^{-1}. Standard deviation calculated from a batch of four experiments.

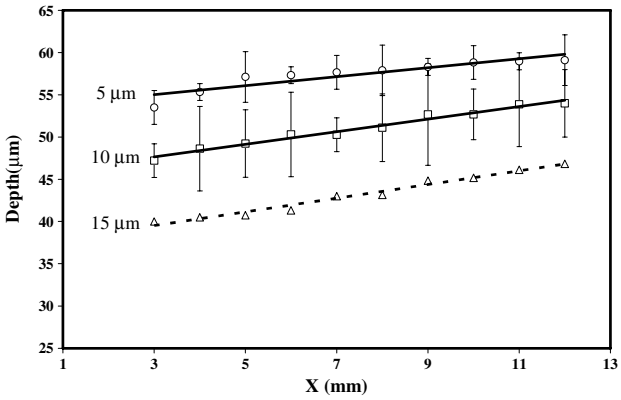

Figure 8. Micro-channel depth profile at different tool distances from the glass surface (machining voltage: 30 V and tool speed: 30 μm s^{-1}). Error bars for 15 μm distance are omitted to improve illustration. Standard deviation calculated from a batch of four experiments.

3.2.4. Influence of the tool distance from the working piece on the micro-channel depth and quality. As discussed in the introduction, 2D micro-machining yields acceptable results when the tool is kept at a distance of less than 25 μm from the glass surface [1]. To study the effect of tool distance on micro-machining performance, several experiments were performed by varying the tool distance from the glass surface. Figure 8 shows the depth profile of the micro-channel machined at 30 V and 30 μm s^{-1} tool speed obtained with different tool distances from the glass surface. The average depth of the micro-channels is observed to decrease with increasing tool distance. The quality of machined micro-channels does not change significantly for tool distances up to 15 μm and, depending on the machining voltage and tool speed, the same contours explained in section 3.1 are observed. For tool distances more than 15 μm, independent of the applied voltage and speed, the micro-channel counters tend to deteriorate as explained in section 3.1.

3.3. Proposal of a model for quality micro-channels as a function of voltage and speed

According to the experimental results discussed in the previous sections for 2D micro-machining with constant velocity using SACE technology, a model based on the observed phenomenon is proposed. Micro-channel fabrication can be divided into five regions in the voltage and tool speed plane, as shown in figure 9.

It is observed that voltages less than 32 V result in better micro-channel quality. In this voltage range, appropriate selection of tool velocity will result in the best micro-channel quality (region 1) in which the channel depth varies between 50 and 120 μm depending on the applied parameters. Lower velocities will result in deeper micro-channels but the quality of the micro-channel edges will not be as good as region 1, although the micro-channel surface quality is still excellent. It should not be neglected that decreasing the speed will change the micro-channel depth smoothly because of the effect of time. So, if the aim is to have a micro-channel with the best quality and a constant depth of around 60 μm the best choice is to apply 28 V at 20 μm s^{-1} speed. In voltages less than 28 V which results in a different electrochemical discharge regime, perfect edge and surface quality are obtained even at tool speeds less than 5 μm s^{-1}. This effect has also been reported for micro-hole drilling by gravity feed [7] and constant feed [16].

In voltages more than 32 V the quality of the micro-channel edges is always heat affected. In this range if the velocity is chosen high enough, it is possible to have smooth micro-channel surfaces which have been indicated as region 3 in figure 9. On the flip side decreasing the tool velocity corrupts the micro-channel surface and results in a very bad

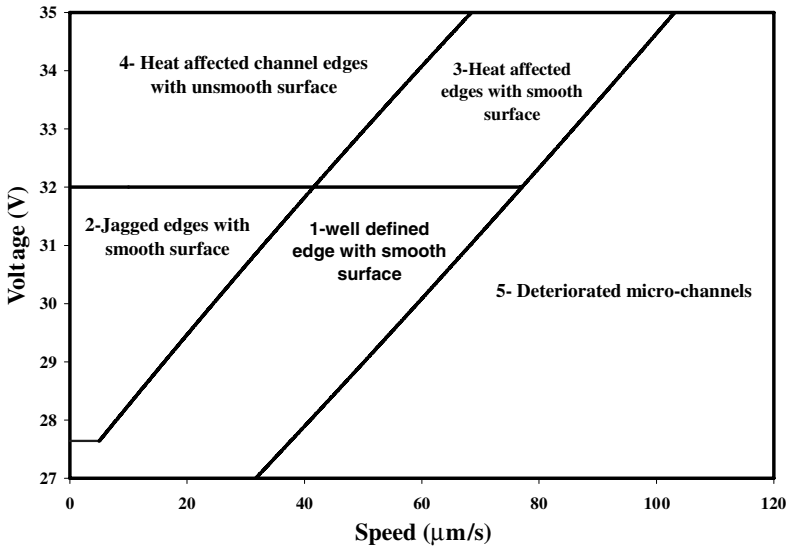

Figure 9. Characterization diagram proposed for micro-channels machined by SACE technology as a function of the applied voltage and speed (for tool distance less than 15 μm).

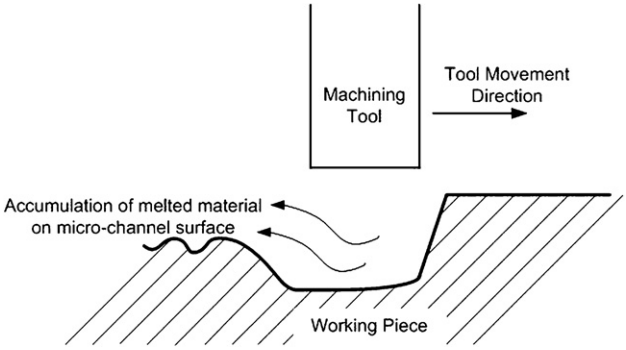

Figure 10. Schematic representation for accumulation of the melted material on the micro-channel surface for higher voltages at low speeds (region 4).

surface quality (region). As mentioned before, this seems to be because of the accumulation of the melted material inside the micro-channel area and inability in removing the melted material from the micro-channel surface. A schematic diagram of this process is shown in figure 10. This is represented by region 4.

Finally, region 5 in figure 9 is a result of excessive speed. In this region there is not enough time for the glass to melt and form an acceptable micro-channel. As the tool is moved above the glass surface with high speeds (region 5), it is possible to see the effect of the tool on the glass during the machining (figure 3(*e*)). In this region machined micro-channels look like discrete rings with 700 μm diameter. When the tool is moved along the micro-channel at lower speeds, these discrete rings combine together to form a continuous micro-channel.

In 2D micro-machining with constant velocity, the machining takes place mostly in the discharge regime and rarely in the transient regime. The width of the micro-channels for a stainless-steel tool of 0.5 mm diameter is approximately 700 μm which is 100 μm more than the radius of the tool for each micro-channel edge. This number is reported to be around 80 μm by Maillard *et al* [7] for the micro-holes drilled with the gravity feed technique in the discharge regime using a stainless-steel tool of 0.4 mm diameter [7]. The drilled micro-holes not deeper than 100 μm (discharge regime) have well-defined cylindrical contours with a smooth surface [7], but in 2D micro-machining as shown in figure 9, the quality of the micro-channels depends on the applied voltage and speed (increasing the voltage or decreasing the speed results in heat-affected or jagged edges), even though machining happens in the discharge regime. This difference between the quality of the obtained micro-holes and micro-channels, which are both machined in the discharge regime, may be attributed to the fact that in the 2D micro-machining with constant velocity, the tool is always moved a certain distance from the glass surface which, in high voltages or low speeds, can destroy the quality of the edges. The main similarity between the proposed model for 2D micro-machining to that proposed for micro-holes is the specific voltage in which significant difference is observed in the quality of the edges. This voltage in both models is equal to 32 V.

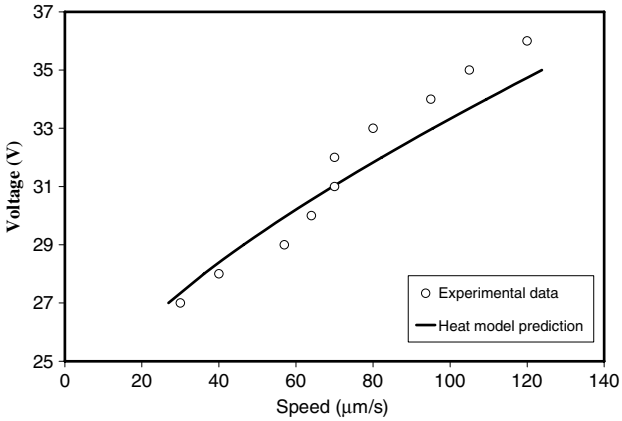

Figure 11. Comparison between experimental data and the proposed theoretical model for the speed limit needed to have micro-channel formation.

3.4. Comparison of experimental data with theory

3.4.1. Heat transfer model and experimental results. Investigation of the time needed for the glass surface to start melting is very important. In figure 9, the boundary of region 5 (deteriorated micro-channels) shows the tool speed in which the glass surface starts to melt for a specific voltage. The time needed for melting the glass surface, assuming 1D heat transfer with a constant homogenous heat source on the glass surface, can be approximated according to equation (1) [17],

$$\overline{T}(z=0,\overline{t_0}) = \sqrt{\overline{t_0}}\left[\frac{1}{\sqrt{\pi}} - \frac{1}{\sqrt{\pi}}\mathrm{e}^{-\frac{1}{\overline{t_0}}} + \frac{1}{\sqrt{\overline{t_0}}}\,\mathrm{erfc}\left(\frac{1}{\sqrt{\overline{t_0}}}\right)\right] = \frac{1}{\kappa}. \tag{1}$$

Simplifying equation (1) to find $\bar{t}_0$ results in

$$\bar{t}_0 = \frac{b^2}{4a}\frac{k^2}{\pi(\kappa-1)^2}, \tag{2}$$

where a is the thermal diffusivity of glass, b is the tool radius and κ is the ratio between the applied heat power and the minimal heat power necessary for machining.

The velocity required to melt a specific length of the glass surface (b' which is about 25 μm according to figure 3(*e*)) is

$$V = \frac{b'}{\bar{t}_0}. \tag{3}$$

Equation (3) indicates the speed at which the glass surface starts to melt. This speed is a representation of the boundary between well-defined micro-channels with smooth surface (region 1 in figure 9) and deteriorated micro-channels (region 5 in figure 9). Figure 11 shows how this simplified heat model is capable of predicting the results for the boundary between regions 1 and 5 proposed in figure 9. According to the experimental data presented in figure 9, there is a jump in tool speed around 32 V. This jump is most probably related to different regimes of electrochemical discharge and gas film formation. Further studies are needed to investigate it.

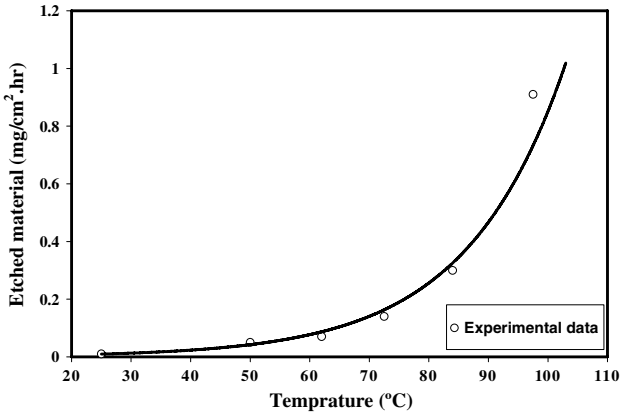

Figure 12. Chemical etching at different temperatures according to Fascio [18].

3.4.2. Chemical etching model and experimental results. As discussed in the previous sections, micro-channel geometry has a specific depth at the beginning of machining and this depth increases with time. Two mechanisms can be proposed for material removal. In the first mechanism, the initial depth of the micro-channels is due to melting of the glass surface and the increasing trend in micro-channels depth is because of chemical etching. Alternatively, machining may happen mainly because of chemical etching at high local temperature. The proposed chemical etching model in this paper is based on the first mechanism. Therefore here we assume that as the machining starts, high temperature melts the glass surface and machines the surface to a specific depth depending on the applied voltage and tool speed. This depth is retained at a constant level along the channel if the only phenomenon contributing to the machining process were physical melting of the glass surface. However high local temperatures will increase the rate of chemical etching, making it a significant contributor to the machining process. Experimental data from Fascio [18] show the relation between the glass etching rate and applied temperature, as illustrated in figure 12.

Fitting the experimental data in figure 12 to the Arrhenius equation form results in the following equation:

$$m = 3 \times 10^7 \exp\left(-\frac{6571.3}{T}\right), \tag{4}$$

where m is the mass of the material removed in 1 h per unit area of the glass and T is the etching temperature. As discussed in section 3.2.1, there is an increasing trend in micro-channels depth with time. Increasing rate in micro-channels depth for different tool speeds has been shown in figure 13(*a*). According to this figure, the increasing rate for micro-channel depth varies as a function of the applied voltage and tool speed. Applied voltage, as a representation of the heat transferred to the glass surface, and tool speed, as a representation of the time in which the tool remains above a specific point, both affect the local temperature of the glass surface. As the thermal energy (applied voltage) or the duration of heat transfer increases (tool speed decreases), the local average temperature at which the chemical etching reaction happens will increase. Therefore the chemical etching rate will also increase according to equation (4). Figure 13(*b*) shows this temperature variation for 28 V in different speeds.

According to Fascio [18] at constant temperature, the mass removed from the glass surface by chemical etching increases at a constant rate. Our experimental data illustrated in figure 13(*a*) also show that increasing rate in micro-channel depth is constant for each specific applied voltage and tool speed. So the constant increasing rate in the machined micro-channel depth can be attributed to the chemical etching which happens at constant temperature. Figure 13(*a*) can be used to control the tool motion in order to cancel the chemical etching effect on micro-channel's depth.

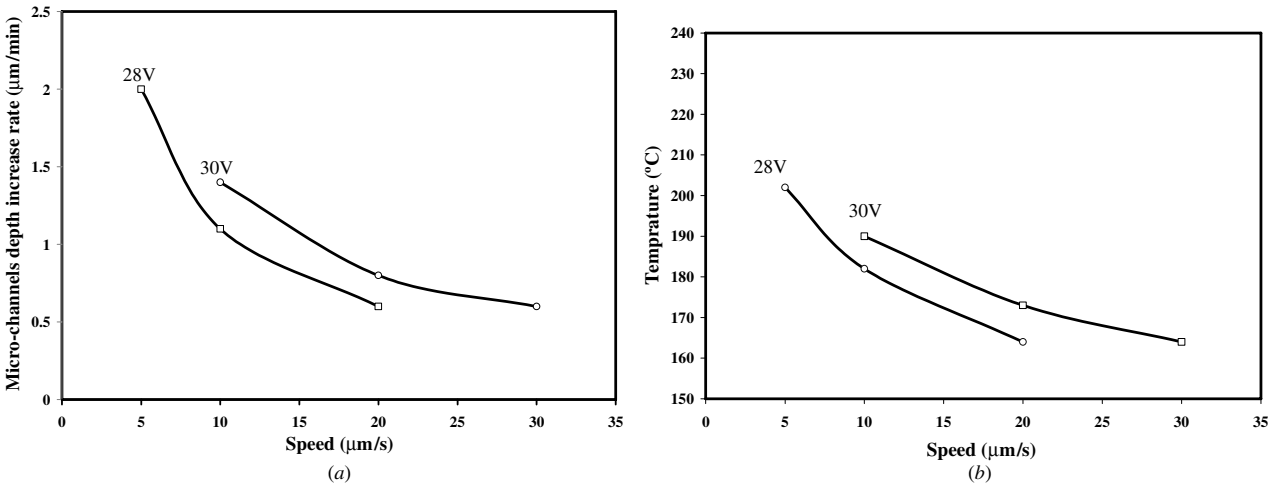

Figure 13. (*a*) Increase in rate of micro-channel depth as a function of tool speed at different voltages, (*b*) predicted local chemical etching temperature at 28 V and 30 V for different tool speeds.

4. Conclusion

Parameters affecting the quality and geometry of micro-channels machined by SACE technology with constant velocity were represented and the effect of each of the parameters was assessed. Meanwhile, using a cylindrical tool with 0.5 mm diameter, the micro-channel width remains constant, around 700 μm, and their depth can vary between 50 and 300 μm depending on different parameters. The best micro-channel quality with desired depth can be achieved with voltages less than 32 V and tool velocity less than 30 μm s^{-1} at a tool distance less than 15 μm from the glass surface.

Five types of micro-channels were obtained:

(1) well-defined linear micro-channel edges and a smooth channel surface;
(2) jagged outline contours with a smooth micro-channel surface;
(3) heat-affected edges with a smooth micro-channel surface;
(4) heat-affected edges with an unsmooth micro-channel surface and thermal cracks;
(5) deteriorated micro-channels.

The presented qualitative model with achievable geometrical properties of the micro-channels, using SACE technology with constant velocity, is a new approach for 2D micro-fabrication which can be used in a lot of applications especially in micro-fluidic and lab-on-chip devices.

This study has drawn our attention to several interesting phenomena such as the effect of chemical etching on machining with SACE technology and predicting the local machining temperature based on the chemical etching rate.

Acknowledgments

This work was supported by the Natural Sciences and Engineering Research Council of Canada (NSERC) and MDEIE-SIIRI (Quebec, Canada).

References

[1] Wüthrich R and Fascio V 2005 Machining of non-conducting materials using electrochemical discharge phenomenon—an overview *Int. J. Mach. Tools Manuf.* **45** 1095–108
[2] Bhattacharyya B, Doloi B N and Sorkhel S K 1999 Experimental investigations into electrochemical discharge machining (ECDM) of non-conductive ceramic materials *J. Mater. Process. Technol.* **95** 145–54
[3] Wüthrich R, Spaelter U and Bleuler H 2006 The current signal in spark-assisted chemical engraving (SACE): what does it tell us? *J. Micromech. Microeng.* **16** 779–85
[4] Jain V K, Choudhury S K and Ramesh K M 2002 On the machining of alumina and glass *Int. J. Mach. Tools Manuf.* **42** 1269–76
[5] Jain V K and Chak S K 2000 Electrochemical spark trepanning of alumina and quartz *Mach. Sci. Technol.* **4** 277–90
[6] Cook N H, Foote G B, Jordan P and Kalyani B N 1972 Experimental studies in electro-machining *ASME* Paper 72-WA/Prod-21
[7] Maillard P, Despont B, Bleuler H and Wüthrich R 2007 Geometrical characterization of micro-holes drilled in glass by gravity-feed with spark assisted chemical engraving (SACE) *J. Micromech. Microeng.* **17** 1343–9
[8] Fascio V, Wuthrich R, Fujisaki K, Viquerat D, Langen H and Bleuler H 2003 Spark assisted chemical engraving: a novel technology for glass microstructuring *European Congress on Advanced Materials and Processes (EUROMAT) (Lausanne)* Invited lecture
[9] Wüthrich R, Fascio V, Viquerat D and Langen H 2002 Study of spark assisted chemical engraving-process technology data *Int. Conf. of the European Society for Precision Engineering and Nanotechnology (EUSPEN) (Eindhoven)* pp 265–8
[10] Wüthrich R 2003 Spark assisted chemical engraving—a stochastic modeling approach *Doctor of Philosophy Thesis* Swiss Federal Institute of Technology (EPFL)
[11] Langen H, Ceausoglu I, Van der Meer M, Lehmann E, Bleuler H and Renaud P 1997 Electrochemical micromachining of glass using Mico-EDMed microtools *Proc. Ultraprecision in Manufacturing Engineering (Braunsweig)* p 672
[12] Wüthrich R, Fascio V, Viquerat D and Langen H 1999 *In situ* measurement and micro-machining of glass *Int. Symp. Micromecatronics and Human Science* pp 185–91
[13] Fascio V, Langen H H, Bleuler H and Comninellis C 2003 Investigations of the spark assisted chemical engraving *Electrochem. Commun.* **5** 203–7
[14] Zheng Z, Cheng W, Huang F and Yan B 2007 3D microstructuring of Pyrex glass using the electrochemical discharge machining process *J. Micromech. Microeng.* **17** 960–6
[15] Han M, Min B and Lee S 2007 Improvement of surface integrity of electro-chemical discharge machining process using powder-mixed electrolyte *J. Mater. Process. Technol.* **191** 224–7
[16] Liao Y and Peng W 2006 Study of hole-machining on Pyrex wafer by electrochemical discharge (ECDM) *Mater. Sci. Forum* **505–7** 1207–12
[17] Maillard P 2008 Investigations on material removal process in SAE glass machining—design of a force measuring set-up *Master's Thesis* Swiss Federal Institute of Technology of Lausanne (EPFL)
[18] Fascio V 2002 Etude de la microstructuration du verre par étincelage assisté par attaque chimique: une approche électrochimique *PhD Thesis* Swiss Federal Institute of Technology of Lausanne (EPFL)